Chemical Bonding in Hypervalent Molecules Revised. 3.† Application of the Atoms in Molecules Theory to Y_3X-CH_2 (X = N, P, or As; Y = H or F) and H_2X-CH_2 (X = O, S, or Se) Ylides

J. A. Dobado,‡ Henar Martínez-García,‡ José Molina Molina,‡,* and Markku R. Sundberg§

Contribution from the Grupo de Modelización y Diseño Molecular, Instituto de Biotecnología, Campus Fuentenueva, Universidad de Granada, E-18071 Granada, Spain, and Laboratory of Inorganic Chemistry, Department of Chemistry, P.O. Box 55 (A.I. Virtasen aukio 1), FIN-00014, University of Helsinki, Finland

Received July 28, 1999. Revised Manuscript Received October 28, 1999

Abstract: The electron pair density in conjunction with the AIM theory and calculated NMR chemical shifts were used to characterize the bonding properties for nine pnicogen and chalcogen ylide structures. The hybrid B3LYP and MP2 methods were employed with the 6-311+G* basis set. No evidence was found to support a banana (Ω) bonding scheme. Instead, different bonding schemes were found to be dependent on the electronegativity of the X atom in the C−X bond. When X is a highly electronegative atom (N,O), the C−X bond is weaker than a single bond, due to electrostatic repulsion. When the X atom has electronegativity similar to carbon, a covalent, yet significantly polar interaction results, and its strength is determined mainly by electrostatic interactions, with a small contribution of negative hyperconjugation.

I. Introduction

Bonding nature on the title ylide compounds has long been controversial,[3,4] and of special interest because of their applications in organic synthesis.[3,5−7] Recently, Gilheany reviewed the chemical bonding in phosphonium ylides.[3] The structure for these complexes is included mainly in the general discussion of other phosphorus hypervalent compounds, especially in chalcogen and pnicogen oxides. In this context, several theoretical bonding definitions for these systems have appeared recently in the literature.[1−3] The application of Atoms in Molecules (AIM) theory has attracted great attention regarding the bonding-nature description of possible hypervalent compounds.[1,2,8]

Bonding studies of phosphonium ylides have been focused on the nature of the C−P bond, and explained in terms of a resonance hybrid between dipolar and double-bonded forms:[9,10]

$$R_3P\oplus - C^{\ominus}H_2 \leftrightarrow R_3P = CH_2 \qquad (1)$$

In early works, the phosphorus d orbitals were considered to be involved in the $d_\pi-p_\pi$ bonding scheme.[9] These $d_\pi-p_\pi$ bond ideas were abandoned based on accurate ab initio calculations on different systems,[11−35] the d functions acting mostly as polarization functions for second-row atoms, compensating for the inflexibility of the sp basis sets. The phosphonium ylide electronic structure has been discussed primarily on the basis of the geometrical parameters described in Figure 1. Moreover, the short C−P bond length and the small τ angle have been considered to support the ylene form. In recent years, highly precise calculations on ylides have been made,[36,37] and the bonding scheme for phosphonium ylides has been defined mainly by the following two alternatives. The first is negative

† For parts 1 and 2, see refs 1 and 2.

* To whom correspondence should be addressed (E-mail: jmolina@ugr.es).
‡ Universidad de Granada.
§ University of Helsinki.

(1) Dobado, J. A.; Martínez-García, H.; Molina, J.; Sundberg, M. R. *J. Am. Chem. Soc.* **1998**, *120*, 8461.
(2) Dobado, J. A.; Martínez-García, H.; Molina, J.; Sundberg, M. R. *J. Am. Chem. Soc.* **1999**, *121*, 3156.
(3) Gilheany, D. G. *Chem. Rev.* **1994**, *94*, 1339.
(4) Burton, D. J.; Yang, Z. Y.; Qiu, W. M. *Chem. Rev.* **1996**, *96*, 1641.
(5) Li, A. H.; Dai, L. X.; Aggarwal, V. K. *Chem. Rev.* **1997**, *97*, 2341.
(6) Cristau, H. J. *Chem. Rev.* **1994**, *94*, 1299.
(7) Padwa, A.; Hornbuckle, S. F. *Chem. Rev.* **1991**, *91*, 263.
(8) Cioslowski, J.; Surján, P. R. *THEOCHEM* **1992**, *255*, 9.
(9) Mitchell, K. A. R. *Chem. Rev.* **1969**, *69*, 157.
(10) Bachrach, S. M. *J. Org. Chem.* **1992**, *57*, 4367.
(11) Wallmeier, H.; Kutzelnigg, W. *J. Am. Chem. Soc.* **1979**, *101*, 2804.
(12) Kutzelnigg, W. *Angew. Chem., Int. Ed. Engl.* **1984**, *23*, 272.
(13) Messmer, R. P. *J. Am. Chem. Soc.* **1991**, *113*, 433.
(14) Kutzelnigg, W. *THEOCHEM* **1988**, *169*, 403.
(15) Reed, A. E.; Schleyer, P. v. R. *J. Am. Chem. Soc.* **1990**, *112*, 1434.
(16) Ehrhardt, C.; Ahlrichs, R. *Theor. Chim. Acta* **1985**, *68*, 231.
(17) Heinzmann, R.; Ahlrichs, R. *Theor. Chim. Acta* **1976**, *42*, 33.
(18) Cruickshank, D. W. J.; Eisenstein, M. *J. Mol. Struct.* **1985**, *130*, 143.
(19) Cruickshank, D. W. J. *J. Mol. Struct.* **1985**, *130*, 177.
(20) Cruickshank, D. W. J.; Eisenstein, M. *J. Comput. Chem.* **1987**, *8*, 6.
(21) Reed, A. E.; Weinhold, F. *J. Am. Chem. Soc.* **1986**, *108*, 3586.
(22) Reed, A. E.; Schleyer, P. v. R. *Chem. Phys. Lett.* **1987**, *133*, 553.
(23) Foster, J. P.; Weinhold, F. *J. Am. Chem. Soc.* **1980**, *102*, 7211.
(24) Reed, A. E.; Weinstock, R. B.; Weinhold, F. *J. Chem. Phys.* **1985**, *83*, 735.
(25) Reed, A. E.; Weinhold, F. *J. Chem. Phys.* **1985**, *83*, 1736.
(26) Cooper, D. L.; Cunningham, T. P.; Gerratt, J.; Karadakov, P. B.; Raimondi, M. *J. Am. Chem. Soc.* **1994**, *116*, 4414.
(27) Gerratt, J.; Lipscomb, W. N. *Proc. Natl. Acad. Sci. U.S.A.* **1968**, *59*, 332.
(28) Cooper, D. L.; Gerratt, J.; Raimondi, M. *Adv. Chem. Phys.* **1987**, *69*, 319.
(29) Cooper, D. L.; Gerratt, J.; Raimondi, M. *Chem. Rev.* **1991**, *91*, 929.
(30) Ladner, R. C.; Goddard, W. A. *J. Chem. Phys.* **1969**, *51*, 1073.
(31) Magnusson, E. *J. Am. Chem. Soc.* **1990**, *112*, 7940.
(32) Magnusson, E. *J. Am. Chem. Soc.* **1993**, *115*, 1051.
(33) Harcourt, R. D. *J. Mol. Struct.* **1992**, *259*, 155.
(34) Harcourt, R. D. *J. Mol. Struct.* **1993**, *300*, 243.
(35) Legon, A. C.; Millen, D. J. *J. Chem. Soc. A* **1968**, 1736.
(36) Naito, T.; Nagase, S.; Yamataka, H. *J. Am. Chem. Soc.* **1994**, *116*, 10080.
(37) Nyulászi, L.; Veszprémi, T. *J. Phys. Chem.* **1996**, *100*, 6456.

10.1021/ja992672z CCC: $19.00
Published on Web 01/26/2000

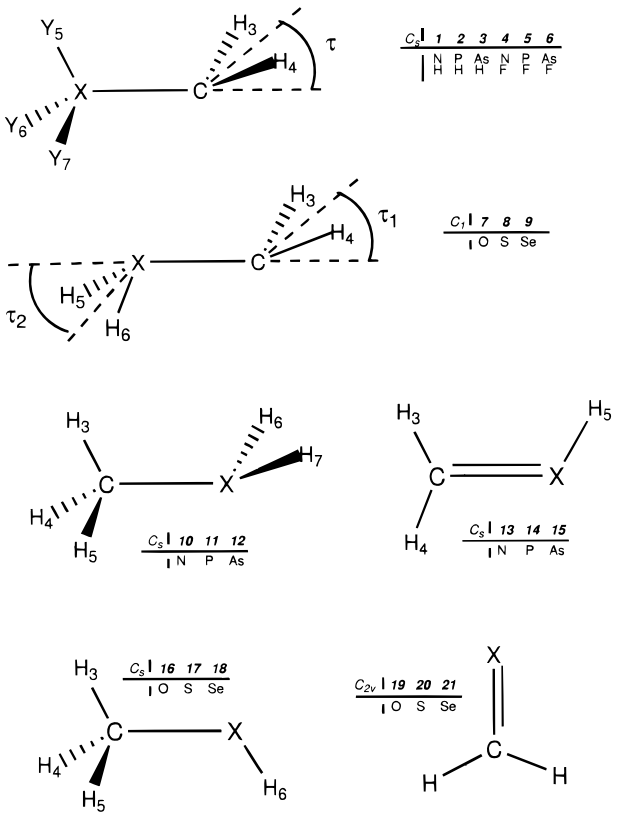

Figure 1. The studied molecules **1**−**9** and the additional molecules **10**−**21** for comparison.

hyperconjugation; in this scheme, the phosphorus lone pair forms a σ bond to carbon, and the extra charge density on carbon forms a π back-bond by overlapping with the σ^* lowest unoccupied molecular orbital (LUMO) of the phosphine moiety.[38] This representation is totally analogous to that proposed for phosphine oxide.[15] The second comprises Ω bonds; this case is also analogous to phosphine oxide, yet yielding only two banana bonds. This situation was also determined by Boys localization procedures in molecular orbital (MO) calculations.[39,40] Moreover, General Valence Bond (GVB) calculations on ylides gave the same results.[41] The above discussion illustrates the controversy between the different wave function analyses.

The gauge-invariant atomic orbital (GIAO) method[42] was employed to calculate NMR data and the results were comparable with experiment; in this context, Chesnut[43] analyzed the bonding in phosphine oxide with the help of theoretical chemical shift calculations.

In the present work, the bonding nature of the title compounds is investigated by performing an adequate analysis of the electron charge density ($\rho(r)$) topology, using the AIM theory recently considered as an appropriate approach that provides a comprehensible set of interpretative tools.[44] The molecules studied (Figure 1) are pnicogen (N, P, As) and chalcogen (O, S, Se) ylides (**1**−**9**), as well as additional compounds for comparison (**10**−**21**). Theoretical calculations for several of the above-mentioned compounds are described in the literature and the most accurate results are summarized in Table 1. To our knowledge, no previous theoretical calculations have been performed for **4** and **6**. The goal of the present work is to describe accurately the bonding nature for the title ylide compounds by means of AIM theory and theoretical NMR chemical shift calculations.

Table 1. Previously Calculated C−X Bond Lengths (Å)

compound	method	C−X
1 H_3N-CH_2	MP2/6-311++G**	1.550[a]
2 H_3P-CH_2	MP2/6-311++G**	1.669[b]
3 H_3As-CH_2	HF/DZ*	1.782[c]
5 F_3P-CH_2	HF/3-21G*	1.590[d]
7 H_2O-CH_2	MP2/6-311++G**	1.734[e]
8 H_2S-CH_2	MP2/DZ*	1.680[f]
9 H_2Se-CH_2	MP2/DZ*	1.790[g]

[a] ref 59 (see also refs 41,60). [b] ref 59 (see also refs 10,38,39,41,60−66). [c] ref 65. [d] ref 62. [e] ref 67 (see also refs 41,60,68,69). [f] ref 70 (see also refs 38,41,60). [g] ref 70.

II. Computational Details

Density functional theory (B3LYP)[45,46] and ab initio (MP2)[47] calculations were performed with the GAUSSIAN 98 package of programs,[48] using the 6-311+G* basis set. The structures presented were fully optimized at the above-mentioned levels of theory, with constrained C_s symmetry for **1**−**6** and **10**−**18**, and C_{2v} for **19**−**21**. Vibrational analyses were used to check the nature of the stationary points, and none of the structures **1**−**21** presented imaginary frequencies (true minima) at either B3LYP or MP2 levels. To study electronic properties, the wave functions for the optimized structures were analyzed by the AIMPAC series of programs[49] using the B3LYP and MP2 densities as input, as described in AIM theory.[51,52] The $\nabla^2\rho(r)$ contour map representations of the different structures were drawn using the MORPHY98 program.[53] The atomic charges were calculated using the AIMPAC series of programs,[49] by integration over the basin of every atom in the AIM's framework. The NMR chemical shifts were calculated with the GIAO method[42] within the GAUSSIAN 98 program,[48] using the tetramethylsilane (TMS) signal as reference for the ^{13}C and ^{1}H chemical shifts.

III. Results and Discussion

A. Geometrical Description. Calculations on structures **1**−**9** were made at the theoretical levels described previously. The

(38) Mitchell, D. J.; Wolfe, S.; Schlegel, H. B. *Can. J. Chem.* **1981**, *59*, 3280.
(39) Molina, P.; Alajarin, M.; Leonardo, C. L.; Claramount, R. M.; Foces-Foces, M. C.; Cano, F. H.; Catalán, J.; de Paz, J. L. G.; Elguero, J. *J. Am. Chem. Soc.* **1989**, *111*, 355.
(40) Bollinger, J. C.; Houriet, R.; Kern, C. W.; Perret, D.; Weber, J.; Yvernault, T. *J. Am. Chem. Soc.* **1985**, *107*, 5352.
(41) Dixon, D. A.; Dunning, T.H.; Eades, R. A.; Gassman, P. G. *J. Am. Chem. Soc.* **1983**, *105*, 7011.
(42) Wolinski, K.; Hilton, J. F.; Pulay, P. *J. Am. Chem. Soc.* **1990**, *112*, 8251.
(43) Chesnut, D. B. *J. Am. Chem. Soc.* **1998**, *120*, 10504.
(44) Cioslowski, J.; Mixon, S. T. *Inorg. Chem.* **1993**, *32*, 3209.
(45) Lee, C.; Yang, W.; Parr, R. G. *Phys. Rev. B* **1988**, *37*, 785.
(46) Becke, A. D. *J. Chem. Phys.* **1993**, *98*, 5648.
(47) Møller, C.; Plesset, M. S. *Phys. Rev.* **1934**, *46*, 618.
(48) Frisch, M. J.; Trucks, G. W.; Schlegel, H. B.; Scuseria, G. E.; Robb, M. A.; Cheeseman, J. R.; Zakrzewski, V. G.; Montgomery Jr., J. A.; Stratmann, R. E.; Burant, J. C.; Dapprich, S.; Millam, J. M.; Daniels, A. D.; Kudin, K. N.; Strain, M. C.; Farkas, O.; Tomasi, J.; Barone, V.; Cossi, M.; Cammi, R.; Mennucci, B.; Pomelli, C.; Adamo, C.; Clifford, S.; Ochterski, J.; Petersson, G. A.; Ayala, P. Y.; Cui, Q.; Morokuma, K.; Malick, D. K.; Rabuck, A. D.; Raghavachari, K.; Foresman, J. B.; Cioslowski, J.; Ortiz, J. V.; Stefanov, B. B.; Liu, G.; Liashenko, A.; Piskorz, P.; Komaromi, I.; Gomperts, R.; Martin, R. L.; Fox, D. J.; Keith, T.; Al-Laham, M. A.; Peng, C. Y.; Nanayakkara, A.; Gonzalez, C.; Challacombe, M.; Gill, P. M. W.; Johnson, B.; Chen, W.; Wong, M. W.; Andres, J. L.; Gonzalez, C.; Head-Gordon, M.; Replogle, E. S.; Pople, J. A.; *Gaussian 98, Revision A.6*; Gaussian Inc.: Pittsburgh, PA, 1998.
(49) Biegler-Köning, F. W.; Bader, R. F. W.; Tang, T. H. *J. Comput. Chem.* **1982**, *3*, 317.
(50) Bader, R. F. W.; Stephens, M. E. *J. Am. Chem. Soc.* **1975**, *97*, 7391.
(51) Bader, R. F. W. *Atoms in Molecules: A Quantum Theory*; Clarendon Press: Oxford, 1990.
(52) Bader, R. F. W. *Chem. Rev.* **1991**, *91*, 893.
(53) MORPHY98, a program written by P. L. A. Popelier with a contribution from R. G. A. Bone, UMIST: Manchester, England, 1998.

Table 2. Geometrical Parameters[a] (Å, Degrees) at the B3LYP/6-311+G*//B3LYP/6-311+G* Level and in Parentheses the MP2/6-311+G*//MP2/6-311+G* Values

	1 H_3N-CH_2	**2** H_3P-CH_2	**3** H_3As-CH_2	**4** F_3N-CH_2	**5** F_3P-CH_2	**6** F_3As-CH_2
C−X	1.563(1.548)	1.681(1.678)	1.836(1.815)	1.287(1.312)	1.616(1.612)	1.788(1.752)
$C-H_3$	1.101(1.098)	1.084(1.084)	1.091(1.090)	1.079(1.079)	1.081(1.080)	1.089(1.087)
$X-Y_5$	1.037(1.027)	1.452(1.438)	1.566(1.551)	1.790(1.721)	1.598(1.585)	1.770(1.748)
$X-Y_6$	1.016(1.014)	1.408(1.402)	1.509(1.504)	1.363(1.357)	1.572(1.563)	1.726(1.711)
$\angle H_2-C-H_3$	106.2(107.3)	115.9(116.2)	111.9(113.4)	124.6(125.0)	119.7(119.9)	115.3(117.7)
$\angle C-X-Y_5$	121.6(120.2)	130.1(129.4)	133.4(131.8)	119.9(121.5)	127.3(126.7)	139.0(135.4)
$\angle C-X-Y_6$	107.4(107.2)	111.9(111.6)	110.2(110.8)	117.6(116.2)	114.2(114.3)	110.8(112.6)
$\angle Y_5XCY_6$	−123.3(−123.0)	−121.2(−121.1)	−123.2(−122.6)	−112.8(−115.1)	−119.0(−119.1)	−123.1(−121.8)
τ	67.5(66.4)	31.5(31.6)	50.6(47.9)	14.3(22.1)	15.31(15.6)	48.2(41.7)

	7 H_2O-CH_2	**8** H_2S-CH_2	**9** H_2Se-CH_2	**10** H_2N-Me	**11** H_2P-Me	**12** H_2As-Me
C−X	1.772(1.688)	1.675(1.663)	1.843(1.820)	1.465	1.872	1.997
$C-H_3$	1.100(1.094)	1.082(1.081)	1.088(1.087)	**13**	**14**	**15**
$C-H_4$	1.106(1.100)	1.084(1.082)	1.087(1.086)	$HN=CH_2$	$HP=CH_2$	$HAs=CH_2$
$X-H_5$	0.967(0.964)	1.423(1.400)	1.566(1.551)	1.267	1.670	1.786
$X-H_6$	0.962(0.958)	1.363(1.354)	1.490(1.484)	**16**	**17**	**18**
$\angle X-C-H_3$	94.8(96.5)	111.1(111.5)	107.9(108.5)	MeOH	MeSH	MeSeH
$\angle X-C-H_4$	96.6(98.6)	119.4(119.8)	115.5(116.2)	1.422	1.834	1.978
$\angle C-X-H_5$	119.7(119.0)	118.9(118.2)	118.7(118.2)	**19**	**20**	**21**
$\angle C-X-H_6$	101.7(104.2)	106.1(107.1)	100.4(101.7)	$H_2C=O$	$H_2C=S$	$H_2C=Se$
$\angle H_3CXH_6$	−156.8(−154.4)	−158.6(−154.7)	−173.2(−169.7)	1.201	1.615	1.776
$\angle H_4XCH_5$	−23.2(−25.6)	−38.7(−39.7)	−35.0(−35.8)			
∠H−X−H	109.8(110.7)	89.4(90.5)	87.4(88.1)			
∠H−C−H	104.4(106.0)	117.5(118.5)	114.2(115.3)			
τ_1	80.4(77.3)	34.6(32.0)	46.9(44.5)			
τ_2	50.8(48.9)	56.3(56.0)	59.6(59.4)			

[a] See Figure 1, the C−X distance was tabulated for structures **10**−**21**.

numerical results are presented in Table 2 together with the C−X bond length for the reference structures (**10**−**21**). Table SI lists the total energies and calculated dipole moments (available as Supporting Information).

As mentioned in the Introduction, the interaction between C and X has been considered to be a ylidene bond, based mainly upon the geometrical parameters. The C−X bond lengths for **2**, **3**, **8** and **9** are closer to their corresponding C−X double bond than to single bonds in the reference compounds. However, compounds **1** and **7** have longer C−X bonds than a normal single bond (1.563 and 1.838 vs 1.465 and 1.422 Å, respectively). Compounds **1** and **7** (where X is nitrogen or oxygen, respectively, with greater electronegativity than the carbon atom) showed behavior similar to that of R_2OO structures,[2] i.e., weaker C−X bond than a normal single bond. On the contrary, the C−X bond length is markedly shortened in compound **1** when nitrogen has three fluorine substituents, giving C−N bond a length very similar to that of a standard C=N double bond. This C−X shortening is also observed for compounds **5** and **6**, but in a very small amount, giving C−P and C−As lengths very close to standard double bonds.

The geometrical agreement of the different structures with the ylidene bond correlates with the τ angle defined in Figure 1. In a pure ylidene form, the τ angle has very small values; however, structures **1** and **7** display the widest angles (67.5 and 80.4°, respectively). Structures **2**, **3**, **8**, and **9** have intermediate values of ca. 40°. The smallest τ angles are found for **4** and **5**, which have three fluorine substituents. The τ values correlate also with the C−H bond lengths. Smaller τ values give shorter bond lengths; the shortest ones are found for **4** (C−H 1.079 Å and τ 14.3°).

The B3LYP geometrical results were also tested with MP2 calculations. Both data match each other with shorter bond lengths and wider bond angles at the MP2 level (Table 2). The geometrical characteristics discussed above lead to the following considerations:

- Structures **1** and **7**, with X=N and O, respectively, show weak C−X bonds, particularly for **7**, with distances longer than standard C−X bonds.[54]
- Structures **2**, **3**, **8**, and **9** show C−X bonds shorter than standard C−X single bonds, with intermediate τ values and considerable ylidene contribution.
- Structures **4**, **5**, and **6**, with three fluorine substituents, present C−X bond lengths very similar to standard double bonds and very small τ values.

B. Bonding Nature. The bonding nature was analyzed by means of the numerical values of the bond critical points (BCP) in $\rho(r)$ and $\nabla^2\rho(r)$ together with the $\nabla^2\rho(r)$ graphical analysis, AIM charges, and electron delocalization between atoms. These analyses were compared with the chemical shifts calculated for **1**−**9** and with the corresponding reference structures (**10**−**21**).

The quantum-mechanical pair density in conjunction with the quantum definition of an atom in a molecule provides a precise determination of the extent to which electrons are localized in a given atom and delocalized over any pair of atoms.[55] The electron pairing is a consequence of the Pauli exclusion principle, and the extent of spatial localization of the pairing is determined by the corresponding property of the Fermi hole density. These ideas are made quantitative through the appropriate integration of the pair density to determine the total Fermi correlation contained within a single atomic basin, the quantity F(A,A), or F(A,B), the correlation shared between two basins. The quantity F(A,B) is thus a measure of the extent to which electrons of either spin referenced to atom A are delocalized onto atom B with a corresponding definition of F(B,A). Thus, F(B,A) = F(A,B) and their sum, F(A,B) + F(B,A) = δ(A,B),

(54) For structure **7**, a C_s conformation was characterized as being 0.7 kcal/mol more stable than the C_1 conformation, at the B3LYP level. In fact, the C−X bond is almost barrierless.

(55) Fradera, X.; Austen, M. A.; Bader, R. F. W. *J. Phys. Chem. A* **1999**, *103*, 304.

Table 3. The Electron Charge Density, $\rho(r)$, its $\nabla^2\rho(r)$, Ellipticity, ϵ, Electronic Energy Density, $E_d(r)$, and $|\lambda_1/\lambda_3|$, of Structures **1**−**21**, for the C−X BCPs at the B3LYP/6-311+G* Theoretical Level

	$\rho(r)$ (e/a_o^3)	$?^2\rho(r)$ (e/a_o^5)	ϵ	E_d(r) (hartree/a_o^3)	$\lvert\lambda_1/\lambda_3\rvert$
1 H_3N-CH_2	0.178	−0.160	0.261	−0.176	0.887
2 H_3P-CH_2	0.193	−0.008	0.441	−0.198	0.600
3 H_3As-CH_2	0.160	−0.116	0.232	−0.106	0.791
4 F_3N-CH_2	0.336	0.138	0.374	−0.508	0.521
5 F_3P-CH_2	0.218	0.143	0.724	−0.233	0.500
6 F_3As-CH_2	0.172	−0.126	0.308	−0.123	0.812
7 H_2O-CH_2	0.093	0.137	0.063	−0.036	0.308
8 H_2S-CH_2	0.217	−0.361	0.366	−0.178	1.453
9 H_2Se-CH_2	0.166	−0.131	0.249	−0.103	0.822
10 H_2N-Me	0.259	−0.650	0.037	−0.267	1.467
11 H_2P-Me	0.150	−0.254	0.094	−0.614	1.804
12 H_2As-Me	0.127	−0.058	0.029	−0.068	0.629
13 $HN=CH_2$	0.387	−0.889	0.192	−0.140	1.176
14 $HP=CH_2$	0.187	0.330	0.391	−0.173	0.341
15 $HAs=CH_2$	0.175	0.048	0.264	−0.126	0.503
16 MeOH	0.251	−0.450	0.009	−0.321	0.997
17 MeSH	0.170	−0.234	0.086	−0.103	0.994
18 MeSeH	0.135	−0.085	0.101	−0.068	0.709
19 $H_2C=O$	0.414	0.080	0.040	−0.696	0.491
20 $H_2C=S$	0.240	−0.105	0.045	−0.302	0.648
21 $H_2C=Se$	0.193	−0.047	0.128	−0.147	0.588

termed the *delocalization index*, is a measure of the total Fermi correlation shared between the atoms (Table 4). This delocalization index is calculated taking into account that

$$F(\mathrm{A,B}) = F(\mathrm{B,A}) = -\sum_i \sum_j S_{ij}(\mathrm{A}) S_{ij}(\mathrm{B}) \qquad (2)$$

where $S_{ij}(A)$ is the corresponding atomic overlap matrix given by the PROAIM program at the Hartree−Fock level.[49,50]

Two different bonding situations arise from the geometrical parameters previously discussed: the first with very weak C−X bonding interactions, where X is highly electronegative N and O (**1** and **7**), and the second characterized by possible C−X multiple bonds.

The AIM atomic charges and NMR chemical shifts for structures **1**−**9** are tabulated in Table 5.

For structure **1**, a weaker bond than a single bond is found according to the BCP numerical values. The electron density, $\rho(r)$, and its Laplacian, $\nabla^2\rho(r)$, have smaller absolute values than in their corresponding C−N single or double bonds for **10** and **13** (0.178 e/a_o^3 and −0.160 e/a_o^5 vs 0.254 e/a_o^3 and −0.650 e/a_o,[5] and 0.387 e/a_o^3 and −0.889 e/a_o,[5] for **1**, **10** and **13**, respectively). Moreover, the local electronic energy density, $E_d(r)$, and the ratio of curvatures, $|\lambda_1/\lambda_3|$, have values close to a covalent bond, but smaller in absolute values than those of a standard single bond for **10**. However, the ellipticity, ϵ, for **1** (0.261) indicates that the $\rho(r)$ varies by a different amount in both directions on the perpendicular plane to the bond. In addition, the electron charge delocalization data (δ[C,N] = 0.92) showed a considerable amount of electron delocalization between the two atoms, and indicated that the elongation of the bonds is also compatible with an electrostatic repulsion due the AIM atomic charges at the N and C atoms (−0.89 and −0.19, respectively).

The above-mentioned trends for **1** appear to be more pronounced for **7**. Thus, the C−O bond lengthens by more than 0.3 Å compared to **16**. The electronic properties of the BCPs suggest a very weak bonding interaction with low $\rho(r)$ and positive $\nabla^2\rho(r)$ values, all indicative of a closed-shell type

Table 4. The Electron Delocalization Indices $\delta[A,B]$ at the B3LYP/6-311+G* Level for Structures **1**−**21**

	1 H_3N-CH_2	**2** H_3P-CH_2	**3** H_3As-CH_2		**4** F_3N-CH_2	**5** F_3P-CH_2	**6** F_3As-CH_2
δ[C,X]	0.92	1.19	1.30	δ[C,X]	1.37	1.14	1.38
δ[C,H_3]	1.00	1.01	1.00	δ[C,H_3]	0.89	0.98	0.96
δ[X,H_5]	0.82	0.73	0.82	δ[X,F_5]	0.51	0.54	0.70
δ[X,H_6]	0.82	0.77	0.91	δ[X,F_6]	1.04	0.54	0.73
δ[C,H_5]	0.08	0.16	0.16	δ[C,F_5]	0.26	0.15	0.14
δ[C,H_6]	0.02	0.11	0.06	δ[C,F_6]	0.09	0.15	0.10
δ[X,H_4]	0.07	0.04	0.06	δ[X,H_4]	0.07	0.04	0.06

	7 H_2O-CH_2	**8** H_2S-CH_2	**9** H_2Se-CH_2		**10** H_2N-Me	**11** H_2P-Me	**12** H_2As-Me
δ[C,X]	0.62	1.48	1.42	δ[C,X]	1.04	0.92	0.99
δ[C,H_3]	1.01	0.98	0.98	δ[C,H_1]	0.94	0.97	0.97
δ[C,H_4]	1.02	0.98	0.98	δ[C,H_4]	0.94	0.98	0.98
δ[X,H_5]	0.66	0.88	0.89	δ[N,H_1]	0.08		
δ[X,H_6]	0.66	0.95	0.98	δ[X,H_6]	0.88	0.90	0.98
δ[C,H_5]	0.01	0.17	0.17	δ[C,H_6]		0.09	
δ[C,H_6]	0.01	0.08	0.07	δ[N,H_4]	0.06		
δ[X,H_3]	0.05	0.07	0.07				
δ[X,H_4]	0.05	0.08	0.07				

	13 $HN=CH_2$	**14** $HP=CH_2$	**15** $HAs=CH_2$		**16** MeOH	**17** MeSH	**18** MeSeH
δ[C,X]	1.79	1.70	1.88	δ[C,X]	0.94	1.13	1.12
δ[C,H_4]	0.92	0.98	0.98	δ[C,H_1]	0.93	0.96	0.96
δ[C,H_5]	0.92	0.98	0.98	δ[C,H_4]	0.94	0.96	0.96
δ[X,H_1]	0.88	0.91	0.99	δ[X,H_6]	0.73	1.05	1.08
δ[N,H_4]	0.10						
δ[C,H_1]		0.16	0.09				
δ[N,H_5]	0.09						

	19 $H_2C=O$	**20** $H_2C=S$	**21** $H_2C=Se$
δ[C,X]	1.59	2.10	2.08
δ[C,H]	0.89	0.95	0.95

Table 5. AIM Atomic Charges and NMR Chemical Shifts[a] for Structures **1**−**21**, at the B3LYP/6-311+G* Theoretical Level

	charge	NMR[a]		charge	NMR[a]		charge	NMR[a]
1 @*C*	−0.19	72.7	**2** @*C*	−1.16	−21.4	**3** @*C*	−0.64	5.8
@*N*	−0.89	201.0	@*P*	2.38	421.7	@*As*	1.18	1462.0
@H_3	−0.03	3.9	@H_3	0.06	−0.7	@H_3	0.05	0.3
@H_5	0.33	5.7	@H_5	−0.44	7.4	@H_5	−0.24	7.6
@H_6	0.40	4.1	@H_6	−0.45	6.3	@H_6	−0.19	5.9
4 @*C*	0.44	98.4	**5** @*C*	−1.26	−0.8	**6** @*C*	−0.57	44.0
@*N*	0.18	−64.2	@*P*	3.25	220.0	@*As*	2.13	955.5
@*H*	0.17	5.2	@*H*	0.12	1.0	@*H*	0.12	2.6
@F_5	−0.50	−599.0	@F_5	−0.74	206.7	@F_5	−0.60	142.5
@F_6	−0.22	−46.6	@F_6	−0.74	259.1	@F_6	−0.60	224.3
7 @*C*	−0.15	278.0	**8** @*C*	−0.40	−4.3	**9** @*C*	−0.51	20.6
@*O*	−0.98	324.1	@*S*	0.29	462.0	@*Se*	0.60	1488.9
@H_3	0.01	12.8	@H_3	0.07	0.7	@H_3	0.05	1.6
@H_4	0.02	12.8	@H_4	0.06	1.2	@H_4	0.05	1.6
@H_5	0.59	2.9	@H_5	−0.04	7.8	@H_5	−0.14	6.5
@H_6	0.56	2.9	@H_6	0.03	7.6	@H_6	−0.06	6.0
10 @*C*	0.27	32.8	**11** @*C*	−0.53	0.7	**12** @*C*	−0.37	0.6
@*N*	−0.98	237.0	@*P*	1.26	465.0	@*As*	0.72	1647.0
@H_3	−0.00	2.8	@H_3	0.04	1.4	@H_3	0.05	1.5
@H_4	0.03	2.6	@H_4	0.04	0.7	@H_4	0.04	0.5
@H_6	0.33	0.2	@H_6	−0.43	3.1	@H_6	−0.24	3.4
13 @*C*	−1.07	167.6	**14** @*C*	−0.95	191.9	**15** @*C*	−0.59	214.0
@*N*	0.63	−119.0	@*P*	1.21	32.5	@*As*	0.67	668.0
@H_3	0.04	8.0	@H_3	0.08	8.6	@H_3	0.09	9.6
@H_4	0.06	7.8	@H_4	0.08	8.4	@H_4	0.08	9.5
@H_5	0.33	10.6	@H_5	−0.42	6.6	@H_5	−0.24	7.0
16 @*C*	0.42	54.2	**17** @*C*	0.13	13.7	**18** @*C*	−0.23	10.0
@*O*	−1.03	314.0	@*S*	−0.06	593.0	@*Se*	0.12	1786.0
@H_3	0.05	3.5	@H_3	0.06	1.6	@H_3	0.06	1.3
@H_4	0.02	3.6	@H_4	0.05	2.1	@H_4	0.06	2.1
@H_5	0.51	−0.5	@H_5	0.02	1.2	@H_5	−0.07	1.9
19 @*C*	0.95	197.1	**20** @*C*	−0.53	258.0	**21** @*C*	−0.34	289.0
@*O*	−1.06	−429.9	@*S*	0.35	−848.0	@*Se*	0.17	−1604.0
@*H*	0.05	10	@*H*	0.09	11.7	@*H*	0.10	12.8

[a] Absolute values except for the ^{13}C and ^{1}H shifts where the TMS signals were used as reference.

interaction compatible with the low absolute values for $|\lambda_1/\lambda_3|$ and $E_d(r)$ (0.308 and −0.036 hartree/a_o^3, respectively). In addition, the δ[C,O] value was small in magnitude (0.62). The forementioned numerical values for **1** and **7** indicate weaker interactions than a normal single bond, yielding for **1**, however, an almost standard covalent bond, whereas **7** is almost a van der Waals complex (see Figure 2). Accordingly, for **1** there is a charge concentration along the bond path, but for **7** there is instead a charge depletion in the bond region.

The calculated NMR chemical shifts are in good accordance with the bonding schemes discussed above for **1** and **7**. Thus, for **1** the ^{15}N shift (201.0 ppm) is closer to that found for **10** (237.0 ppm), also yielding closer ^{13}C values (72.7 and 32.8 ppm, for **1** and **10**, respectively). These values are completely different from those reported for **13** (with a C═N double bond with 167.6 and −119.0 ppm, for ^{13}C and ^{15}N, respectively). For **7**, the ^{17}O and ^{13}C chemical shifts are different from those in **16** and **19**, and with contradictory trends. In addition, the shifts for **7** go in the direction expected for a van der Waals complex, compared to methylene (1372.9 ppm for ^{13}C and 56.9 ppm for ^{1}H) and to water (317.7 ppm for ^{17}O and 0.4 ppm for ^{1}H).

The bonding nature in **1** changes dramatically when three fluorine atoms are bonded to nitrogen (**4**). The methylene moiety becomes almost planar (τ =14.3°), and the $\rho(r)$ at the BCP increases, also giving a positive $\nabla^2\rho(r)$ value but in the same range. Moreover, the ϵ, $E_d(r)$, and $|\lambda_1/\lambda_3|$ increase, indicating a stronger covalent bond with multiple bond character. All of the above matched well with the first alternative mentioned in the Introduction (negative hyperconjugation) if the following is considered.

The C−F_5 bond lengthens by more than 0.4 Å with respect to the C−F_6 bond. This elongation is compatible with the δ[N,F_5] value compared to δ[N,F_6] (0.51 and 1.04, respectively). In addition, δ[C,N] = 1.37 indicates that more than one electron pair is delocalized between them, and δ[C,F_5] = 0.26 shows a larger delocalization for the nonbonded C and F_5 atoms than for the C and F_6 (δ[C,F_6] = 0.09).

All of the above-mentioned results confirm the first alternative and corroborate a considerable C═N double-bond character for **4**. The NMR chemical shifts for **4** (98.4 and −64.2 ppm for ^{13}C and ^{15}N, respectively) approach to that found in **13**. The main differences in the electronic structures are observed when the $\nabla^2\rho(r)$ contour plots for both compounds (**1** and **4**, see Figure 2) are compared.

The bonding nature of compounds **2** and **3** and their corresponding fluorine derivatives have very similar behavior. From a geometrical standpoint the C−X bond acts as a double bond; however, the electronic numerical data indicated that these bonds are not compatible with a standard double bond. The C−X BCPs present values typical for a covalent, yet significantly polar bond. A comparison of the $\rho(r)$ and ϵ gave similar values than those for **14** and **15**, with formal C═X bonds.[56] However, a large deviation appeared in $\nabla^2\rho(r)$. The results for the fluoro derivatives do not change significantly in comparison to **2** and **3** (the geometrical data follow the same trend and the different X−F bond lengths have small differences). The AIM atomic charges for carbon are always large and negative, and their values do not change appreciably in **2** and **3** from the corresponding fluorinated analogues (**5** and **6**). In addition, the X atoms have large and positive charges for **2**, **3**, **5**, and **6**. All of the above is compatible with a very strong electrostatic interaction.

(56) Nyulászi, L.; Szieberth, D.; Réffy, J.; Veszprémi, T. *THEOCHEM* **1998**, *453*, 91.

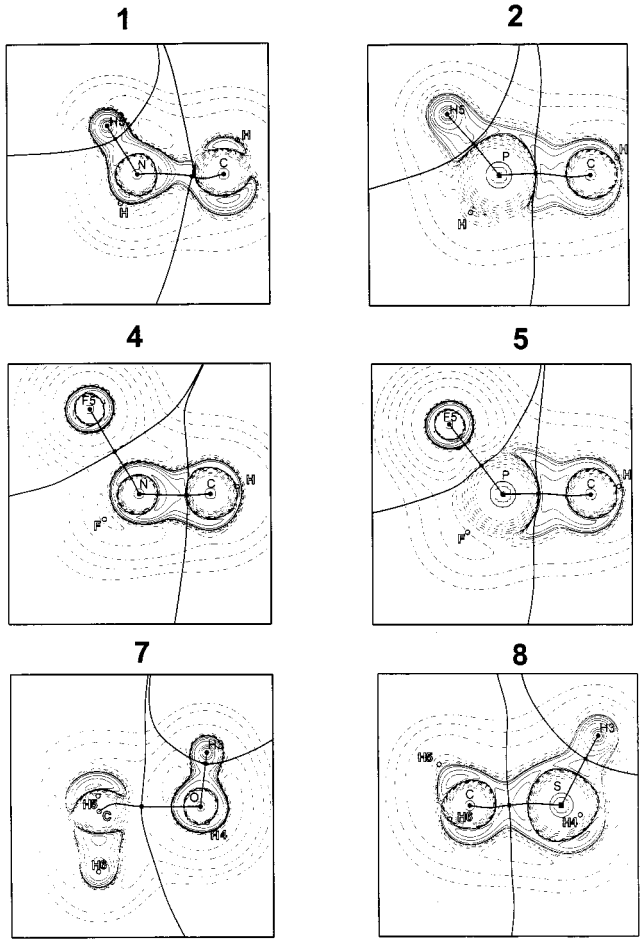

Figure 2. $\nabla^2\rho(r)$ contour maps, in the molecular plane, using the MORPHY98 program,[53] for structures **1**, **2**, **4**, **5**, **7** and **8** calculated at the B3LYP/6-311+G* level. The contours begin at zero and increase (solid contours) and decrease (dashed contours) in steps of ±0.02, ±0.04, ±0.08, ±0.2, ±0.4, ±0.8, ±2.0, ±4.0, ±8.0. The thick solid lines represent the molecular graph that joins the nuclei (solid circles) and the BCP (solid squares), and also represent the zero-flux surface.

The δ[C,X] indices give values slightly larger than 1.0 and remain also unchanged for the fluorinated structures. Thus, the δ[X,H] and δ[X,F] indices are similar for the three X−H or X−F bonds, with only a slight difference appearing in one bond due to a markedly small amount of negative hyperconjugation contribution. The results define a bond very different from a standard double bond, as the NMR results indicate. The ^{13}C chemical shifts appear at a very high field for **2**, **3**, **5**, and **6**, yielding values in all cases substantially different from a standard ^{13}C sp^2 shift (−21.4, 5.8, −0.8, and 44.0 ppm, for **2**, **3**, **5**, and **6**, respectively, compared to 191.9 and 214.0 ppm for **14** and **15**, respectively). Moreover, the X chemical shifts are closer to their respective single-bonding values (see Table 5). These trends are illustrated in Figure 2 for the $\nabla^2\rho(r)$ contour plots of **2** and **5**. A similar representation for **3** and **6** is available as Supporting Information (Figure S1).

Structures **8** and **9** also present geometrical features resembling the ylidene compounds, giving $\rho(r)$ values in agreement with those of **20** and **21**. In addition, the δ[C,X] indices (1.48 and 1.42 for **8** and **9**, respectively) also corroborate a clear large multiple-bond character. However, the other electronic numerical values have the same trend as those calculated for **2** and **3**. This bond is covalent, yet significantly polar with large $\rho(r)$, negative $\nabla^2\rho(r)$ and large $|\lambda_1/\lambda_3|$ values. Furthermore, the charges on the C and X atoms were intermediate (ca. 0.5) and with the opposite signs, also yielding appreciable electrostatic interactions.

The NMR shift values for **8** and **9** are clearly closer to standard single-bonded atom shifts.

The $\nabla^2\rho(r)$ contour plots for **8** are also presented in Figure 2.[57] A maximum of electron charge concentration along the C−X bond is clearly observed for **1**, **2**, **4**, **5**, and **8**, and is completely incompatible with the second alternative presented in the Introduction.

IV. Conclusions

When X is a highly electronegative atom, the C−X bond is weaker than a single bond, owing to electrostatic repulsion. However, the presence of fluorine atoms in **1** reinforces the C−X bond due to a negative hyperconjugation (double-bond contribution).

When the X atom has electronegativity similar to that of carbon, a covalent, yet significantly polar interaction results in and is governed mainly by electrostatic interactions, with a small contribution of negative hyperconjugation, the bonding nature for the fluorinated derivatives (**5** and **6**) remaining.

The chalcogen (S, Se) derivatives have a similar bonding nature, although the electrostatic interaction is weaker (there is a larger electronic delocalization).

When fluorine atoms are replaced by hydrogen atoms in the chalcogen (O, S, or Se) compounds, the bonding description changes completely, as was depicted elsewhere,[58] yielding structures compatible with a three-center, four-electron bonding scheme.

The results of this work do not support a banana (Ω) bonding nature for the studied compounds.

Acknowledgment. Computing time was provided by the Universidad de Granada (Spain). We are grateful to Professor R. F. W. Bader for a copy of the AIMPAC package of programs. M.R.S. thanks Ella och Georg Ehrnrooths Stiftelse for a grant. We thank David Nesbitt for reviewing the language of the original English manuscript.

Supporting Information Available: Table SI: Total energies and dipole moments for structures **1**−**9**. Table SII: parameters in the $\nabla^2\rho(r)$ maxima for structures **1**−**9** (PDF). Figure S1: $\nabla^2\rho(r)$ contour maps, in the molecular plane, using the MORPHY98 program,[53] for structures **3**, **6**, and **9**. This material is available free of charge via the Internet at http://pubs.acs.org. See any current masthead page for ordering information and Web access instructions.

JA992672Z

(57) The $\nabla^2\rho(r)$ contour plots for **9** are similar to those for **8** in Figure 2, and are also available as Supporting Information Figure S1.

(58) Dobado, J. A.; Martínez-García, H.; Molina, J. *Inorg. Chem.* **1999**, *38*, 6257.
(59) Platts, J. A.; Howard, S. T. *J. Chem. Soc., Perkin Trans. 2* **1997**, 2241.
(60) Yates, B. F.; Bouma, W. J.; Radom, L. *J. Am. Chem. Soc.* **1987**, *109*, 2250.
(61) Nyulászi, L.; Veszprémi, T.; Réffy, J. *J. Phys. Chem.* **1995**, *99*, 10142.
(62) Francl, M. M.; Pellow, R. C.; Allen, L. C. *J. Am. Chem. Soc.* **1988**, *110*, 3723.
(63) Streitwieser, A.; Rajca, A.; McDowell, R. S.; Glaser, R. *J. Am. Chem. Soc.* **1987**, *109*, 4184.
(64) Dixon, D. A.; Smart, B. E. *J. Am. Chem. Soc.* **1986**, *108*, 7172.
(65) Strich, A. *Nov. J. Chim.* **1979**, *3*, 105.
(66) Hoffmann, R.; Boyd, D. B.; Goldberg, S. Z. *J. Am. Chem. Soc.* **1970**, *92*, 3929.
(67) Gonzalez, C.; Restrepo-Cossio, A.; Márquez, M.; Wiberg, K. B. *J. Am. Chem. Soc.* **1996**, *118*, 5408.
(68) Zub, L. L.; Standard, J. M. *THEOCHEM* **1996**, *368*, 133.
(69) Tucker, J. M.; Standard, J. M. *THEOCHEM* **1998**, *431*, 193.
(70) Shimizu, T.; Matsuhisa, A.; Kamigata, N.; Ikuta, S. *J. Chem. Soc., Perkin Trans. 2* **1995**, 1805.